Asian Journal of Chemistry; Vol. 38, No. 11 (2026), 3002-3010
ASIAN JOURNAL OF CHEMISTRY
https://doi.org/10.14233/ajchem.2026.36669

Synthesis, Characterization, Molecular Docking and *in vitro* Anti-Breast and Antibacterial Activities of 1-(Naphthalene-6-yl)ethanone Derivatives

EZHILARASI MUTHUVEL RAMANATHAN[1,*], MANJU MATHEW[2] and A. PRINCE RAJA[2]

[1]Department of Chemistry, Dr. N.G.P. Arts and Science College, Coimbatore-641048, India
[2]Department of Chemistry, Karpagam Academy of Higher Education, Coimbatore-641021, India

*Corresponding author: E-mail: ezhilarasi.mr@drngpasc.ac.in

Received: 20 June 2026 *Accepted*: 9 October 2026 *Published online*: 13 November 2026 AJC-22531

A novel series of naphthalene substituted chalcone derivatives containing cyclohexanone compounds moieties (**ANCH 1-2**,**4-8**) was designed, synthesized and evaluated for anticancer activities against the human cancer cell lines like MCF-7 (breast) by employing MTT assay. The anticancer assay identified ANCH-4 as a potential growth inhibitor of tumor cells, with an IC_{50} value of 33 ± 1.8 μM and relatively low toxicity toward the tested human cell line compared with the standard drug. Molecular docking of **ANCH-1**, **ANCH-2** and **ANCH-4-8** was performed against bacterial proteins 1UAG, 5KEE and 5XZ0, along with the breast cancer-associated protein 1OQA. Among the tested compounds, ANCH-2 recorded docking scores of -9.4 kcal/mol against 1UAG, -10.4 kcal/mol against 5KEE and -9.1 kcal/mol against 1OQA, which suggest favourable interactions with the selected protein targets. The compounds displayed interactions within the target binding sites, with their binding patterns compared against those of the corresponding co-crystallized ligands. Finally, *in silico* predictions of ADME and pharmacokinetic parameters indicated that all these compounds **ANCH 1-2** and **4-8** could be considered drug candidates with oral bioavailability.

Keywords: Naphthalene, Chalcone, Cyclohexanone, MDA-MCF-7 cell line.

INTRODUCTION

Chalcones are an important class of compounds characterized by two aromatic rings joined through an α,β-unsaturated carbonyl linkage. This structural arrangement provides a useful framework for chemical modification and has been associated with diverse pharmacological activities, particularly anticancer effects [1,2]. Modifications in the aromatic ring substitution and the attachment of additional functional groups can influence the biological activity and physico-chemical characteristics of chalcone derivatives [3-5]. In this context, cyclohexane-1,3-dione represents an interesting structural component for further molecular modification. Its synthetic versatility and biological potential have attracted attention, with Michael addition serving as one of the approaches used for preparing related derivatives [5]. Combining chalcone and cyclic diketone structural features within the same molecular framework may provide access to new derivatives with distinct chemical properties and biological profiles, justifying systematic design, synthesis, characterization and biological evaluation.

Breast cancer remains a major contributor to cancer incidence and cancer-related mortality among women worldwide [6]. Estrogen receptor signaling is central to the progression of hormone-responsive breast cancer, whereas triple-negative breast cancer (TNBC) is characterized by the absence of estrogen receptor, progesterone receptor and HER2 expression. TNBC presents particular therapeutic challenges and is associated with limited targeted treatment options [7-9]. Dysregulation of cell-cycle control and apoptosis is frequently observed in cancer cells, making these pathways important targets for anticancer drug development [10]. The conventional chemotherapy and hormonal treatments can cause adverse effects, partly through their toxicity toward normal cells [11,12]. The search for compounds with selective anticancer activity and improved safety profiles remains an important area of research [13].

In present study, a series of naphthalene-substituted chalcone derivatives incorporating cyclohexanone or cyclohexane-1,3-dione moieties was designed and synthesized. The synthesized derivatives were designed by integrating the

This is an open access journal, and articles are distributed under the terms of the Attribution 4.0 International (CC BY 4.0) License. This license lets others distribute, remix, tweak, and build upon your work, even commercially, as long as they credit the author for the original creation. You must give appropriate credit, provide a link to the license, and indicate if changes were made.

chalcone framework with a naphthalene ring and a cyclic ketone moiety to examine their influence on biological activity. Antimicrobial activity was examined by the agar disc diffusion method, while the anticancer potential of the compounds was assessed using the MTT assay against the MDA-MB-231 human breast cancer cell line. Molecular docking studies were performed against the selected bacterial protein targets 1UAG, 5KEE and 5XZ0, as well as the cancer-related protein 1OQA, to examine the predicted binding modes and molecular interactions of the synthesized compounds.

EXPERIMENTAL

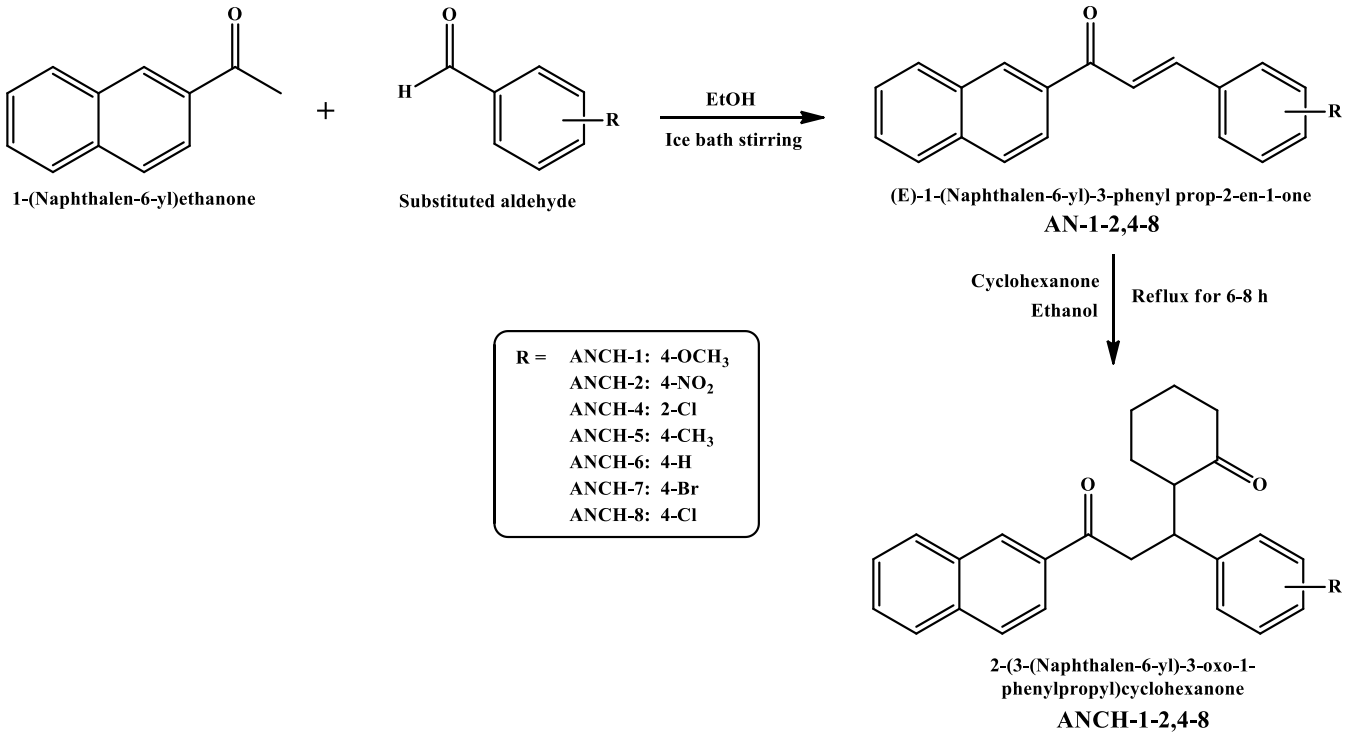
Mostly chemicals and solvents were purchased from Sigma-Aldrich, USA. The melting points of the compounds **ANCH 1-2** and **4-8** were determined using the open capillary method and the values were uncorrected. The FT-IR spectrum (cm^{-1}) was recorded through KBr in an FT-IR spectrometer (model Shimadzu 8400s) in the range of 4000-400 cm^{-1}. The ^1H and ^{13}C NMR spectra were recorded by Bruker 400 and 100 MHz, respectively spectrometer. The chemical shifts were recorded in value (ppm) with TMS as an internal standard as well as $CDCl_3$ used as a solvent.

Synthesis: Naphthyl chalcone derivatives (**AN 1-2** and **AN 4-8**; 0.1 mol) were dissolved in ethanol (30 mL) in a round-bottom flask followed by the addition of cyclohexanone (0.1 mol) and sodium acetate (1 mol). The reaction mixture was stirred under the specified reaction conditions, and its progress was monitored by thin-layer chromatography (TLC). Upon completion, the reaction mixture was poured into a 500 mL beaker containing crushed ice and left overnight at room temperature (**Scheme-I**). The resulting solid was collected by filtration, dried and recrystallized from ethanol [14]. The purity of the synthesized compounds was assessed by TLC using $CHCl_3$ as developing solvent.

2-[1-(4-Methoxy-phenyl)-3-naphthalen-2-yl-3-oxo-propyl]cyclohexanone (**ANCH-1):** Yellow solid; yield: 82%; m.p.: 352.62 ºC; Elemental analysis of $C_{26}H_{26}O_3$ (m.w.: 386.48); calcd. (found) %: C, 80.72 (80.80); H, 6.73 (6.78); O, 12.42 (12.42); IR (KBr, ν_{max}, cm^{-1}): 3042.43, 3027.48 (Ar–CH), 2956.34, 2925.16 (aliphatic C–H), 1724 (C=O); ^1H NMR (400 MHz, $CDCl_3$, δ ppm): 1.008-2.313 (m, cyclohexanone ring protons), 3.099-3.847 (m, aliphatic chain protons), 6.926-8.516 (arom. protons), 2.78 (OCH_3 substituent signal); ^{13}C NMR (100 MHz, $CDCl_3$, δ ppm): 20.98 (C-4), 21.423 (C-5), 29.12 (C-6), 39.26 (C-3), 48.65 (C-2′, aliphatic chain), 51.82 (C-1′, aliphatic chain), 54.23 (substituent carbon), 55.63 (C-1), 114.67-144.84 (arom. carbons), 190.52 (C=O), 201.62 (C=O).

2-[3-Naphthalen-2-yl-1-(4-nitro-phenyl)-3-oxo-propyl]-cyclohexanone (**ANCH-2):** Brown solid; yield: 75%; m.p.: 392.26 ºC; Elemental analysis of $C_{25}H_{23}NO_4$ (m.w.: 401.46); calcd. (found) %: C, 74.79 (74.81); H, 5.78 (5.82); N, 3.49 (3.42); O, 15.94 (15.98); IR (KBr, ν_{max}, cm^{-1}): 3062.36, 3073.14 (Ar–CH), 2932.81, 2915.98 (aliphatic C–H), 1732 (C=O); ^1H NMR (400 MHz, $CDCl_3$, δ ppm): 0.784-1.628 (m, cyclohexanone ring protons), 3.593-3.634 (m, aliphatic chain protons), 6.957-8.432 (arom. protons); ^{13}C NMR (100 MHz, $CDCl_3$, δ ppm): 21.30 (C-4), 21.79 (C-5), 30.97 (C-6), 40.79 (C-3), 47.270 (C-2′, aliphatic chain), 51.944 (C-1′, aliphatic chain), 54.63 (C-1), 121.41-145.17 (arom. carbons), 190.70 (C=O), 202.87 (C=O).

2-[1-(2-Chloro-phenyl)-3-naphthalen-2-yl-3-oxo-propyl]-cyclohexanone (**ANCH-4):** Yellow solid; yield: 82%; m.p.: 349.04 ºC; Elemental analysis of $C_{25}H_{23}ClO_2$ (m.w.: 390.90); calcd. (found) %: C, 76.74 (76.81); H, 5.88 (5.93); O, 8.19



Scheme-I: Synthetic route for the target compounds **ANCH 1-2,4-8**

(8.19); Cl, 9.08 (9.07); IR (KBr, ν_{max}, cm^{-1}): 3054.43, 3032.57 (Ar–CH), 2915.27, 2871.48 (aliph. C–H), 1716.52 (C=O); ^{1}H NMR (400 MHz, $CDCl_3$, δ ppm): 1.129-1.63 (m, cyclohexanone ring protons), 3.395-3.683 (m, aliph. chain protons), 7.254-8.106 (arom. protons); ^{13}C NMR (100 MHz, $CDCl_3$, δ ppm): 21.19 (C-4), 21.43 (C-5), 29.51 (C-6), 37.18 (C-3), 45.13 (C-2′, aliph. chain), 47.60 (C-1′, aliph. chain), 53.91 (C-1), 122.77-143.47 (arom. carbons), 131.8 (substituent carbon), 190.21 (C=O), 199.40 (C=O).

2-(3-Naphthalen-2-yl-3-oxo-1-*p*-tolyl-propyl)cyclohexanone (**ANCH-5):** Pale yellow solid; yield: 85%; m.p.: 330.39 ºC; Elemental analysis of $C_{26}H_{26}O_2$ (m.w.: 370.48); calcd. (found) %: C, 84.21 (84.29); H, 7.02 (7.07); O, 8.64 (8.64); IR (KBr, ν_{max}, cm^{-1}): 3052.76, 3023.84 (Ar–CH), 2956.34, 2925.48 (aliph. C–H), 1706 (C=O); ^{1}H NMR (400 MHz, $CDCl_3$, δ ppm): 1.003-2.408 (m, cyclohexanone ring protons), 3.098-3.783 (m, aliphatic chain protons), 6.937-8.534 (arom. protons), 2.92 (CH_3 substituent signal); ^{13}C NMR (100 MHz, $CDCl_3$, δ ppm): 21.32 (C-4), 21.59 (C-5), 27.75 (methyl carbon), 29.35 (C-6), 41.11 (C-3), 48.91 (C-2′, aliph. chain), 51.56 (C-1′, aliph. chain), 55.97 (C-1), 113.69-155.16 (arom. carbons), 192.19 (C=O), 201.67 (C=O).

2-(3-Naphthalen-2-yl-3-oxo-1-phenyl-propyl)cyclohexanone (**ANCH-6):** Straw-yellow solid; yield: 88%; m.p.: 306.6 ºC; Elemental analysis of $C_{25}H_{24}O_2$ (*m.w.*: 356.46); calcd. (found) %: C, 84.15 (84.24); H, 6.73 (6.79); O, 8.98 (8.98); IR (KBr, ν_{max}, cm^{-1}): 3019.28, 3023.84 (Ar–CH), 2961.34, 2952.48 (aliph. C–H), 1725.41 (C=O); ^{1}H NMR (400 MHz, $CDCl_3$, δ ppm): 1.112-1.346 (m, cyclohexanone ring protons), 3.182-3.762 (m, aliph. chain protons), 7.248-8.534 (arom. protons); ^{13}C NMR (100 MHz, $CDCl_3$, δ ppm): 21.19 (C-4), 21.38 (C-5), 29.15 (C-6), 40.67 (C-3), 48.196 (C-2′, aliph. chain), 51.62 (C-1′, aliph. chain), 53.93 (C-1), 122.39-145.01 (arom. carbons), 190.54 (C=O), 201.92 (C=O).

2-[1-(4-Bromo-phenyl)-3-naphthalen-2-yl-3-oxo-propyl]-cyclohexanone (**ANCH-7):** Brown solid; yield: 74%; m.p.: 378.92 ºC; Elemental analysis of $C_{25}H_{23}BrO_2$ (m.w.: 435.35); calcd. (found) %: C, 68.11 (68.97); H, 5.28 (5.33); O, 7.35 (7.35); Br, 18.38 (18.35); IR (KBr, ν_{max}, cm^{-1}): 3072.78, 3023.54 (Ar–CH), 2916.34, 2825.48 (aliph. C–H), 1705.63 (C=O); ^{1}H NMR (400 MHz, $CDCl_3$, δ ppm): 1.121-1.619 (m, cyclohexanone ring protons), 3.179-3.719 (m, aliph. chain protons), 7.536-8.529 (arom. protons); ^{13}C NMR (100 MHz, $CDCl_3$, δ ppm): 21.19 (C-4), 21.42 (C-5), 28.16 (C-6), 40.19 (C-3), 50.98 (C-1′, aliph. chain), 50.98 (C-2′, aliph. chain), 53.82 (C-1), 121.87-143.55 (arom. carbons), 190.31 (C=O), 202.65 (C=O).

2-[1-(4-Chloro-phenyl)-3-naphthalen-2-yl-3-oxo-propyl]-cyclohexanone (ANCH-8): Yellow solid; yield: 76%; m.p.: 349.04 ºC; Elemental analysis of $C_{25}H_{23}ClO_2$ (m.w.: 390.90); calcd. (found) %: C, 76.74 (76.81); H, 5.88 (5.93); O, 8.19 (8.19); Cl, 9.08 (9.07); IR (KBr, ν_{max}, cm^{-1}): 3048.34, 3015.79 (Ar–CH), 2873.34, 2928.78 (aliph. C–H), 1732.11 (C=O); ^{1}H NMR (400 MHz, $CDCl_3$, δ ppm): 1.131-1.669 (m, cyclohexanone ring protons), 3.395-3.699 (m, aliph. chain protons), 7.404-8.529 (arom. protons); ^{13}C NMR (100 MHz, $CDCl_3$, δ ppm): 21.13 (C-4), 21.31 (C-5), 28.70 (C-6), 33.74 (substituent-associated signal), 38.32 (C-3), 47.60 (C-2′, aliphatic chain), 51.84 (C-1′, aliphatic chain), 54.30 (C-1), 122.77-143.47 (arom. carbons), 132.82 (substituent-associated signal), 190.21 (C=O), 199.29 (C=O).

Antimicrobial screening: The antimicrobial activity was evaluated using the disc diffusion method according to previously reported procedures [15-18]. Nutrient agar (2.8 g) was dissolved in 100 mL of distilled water by heating and 6 mL of the medium was dispensed into each clean Petri dish. The medium was sterilized by autoclaving for 15 min and allowed to solidify. Fresh microbial cultures were prepared by transferring the bacterial strains from stock cultures to nutrient agar slants using a sterile inoculating loop, followed by incubation at 30 ºC for 16 h. Sterile discs impregnated with 20 µL of 10% DMSO served as the negative control, while standard antimicrobial agents were used as positive controls for the bacterial and fungal strains. The test discs were impregnated with 20 µL of each compound solution and placed on the agar plates. The plates were incubated in an inverted position at 30 ºC for 24 h. Antimicrobial activity was assessed by measuring the diameter of the inhibition zones around the discs and the results were expressed in millimetres (mm).

Anticancer activity: MCF-7 human breast adenocarcinoma cells were procured from the National Centre for Cell Science (NCCS), Pune, India and cultured in Dulbecco's Modified Eagle Medium (DMEM; Sigma-Aldrich, USA) supplemented with 10% fetal bovine serum (FBS), L-glutamine, sodium bicarbonate and an antibiotic solution. The cells were maintained at 37 ºC in a humidified incubator containing 5% CO_2. The cell viability was assessed by microscopic observation and the MTT assay. For the anticancer assay, 15 mg of MTT was dissolved in 3 mL of phosphate-buffered saline (PBS) and sterilized by filtration. After 24 h of treatment, the medium was removed and 30 µL of the MTT solution was added to each test and cell control well. The plate was gently shaken and incubated at 37 ºC under 5% CO_2 for 4 h. The supernatant was then removed and 100 µL of MTT solubilization solution was added to each well to dissolve the formazan crystals. Absorbance was measured at 540 nm using a microplate reader [19-21].

ADME studies: The absorption, distribution, metabolism and excretion (ADME) profiles of the synthesized derivatives were predicted using the SwissADME online tool. The analysis includes molecular weight (MW), hydrogen-bond acceptors (HBA), hydrogen-bond donors (HBD), the octanol-water partition coefficient (log P), aqueous solubility (log S), topological polar surface area (TPSA), molar refractivity (MR) and bioavailability score. These descriptors were examined to assess drug-likeness and estimate the potential pharmacokinetic properties of the synthesized compounds [22].

Molecular docking studies: Molecular docking studies were carried out for synthesized **ANCH 1-2** and **4-8** derivatives by bacterial protein and breast cancer protein using Autodock version 4.2.5.1 docking software. The reference method was adopted for the docking study [23-26].

RESULTS AND DISCUSSION

The target compounds **ANCH-1**, **ANCH-2** and **ANCH-4-8** were synthesized through the reaction of the corresponding naphthyl chalcone derivatives with cyclohexanone, as

outlined in **Scheme-I**. The precursor chalcones were obtained by Claisen-Schmidt condensation of substituted benzaldehydes with 1-(naphthalen-6-yl)ethanone. The final compounds were purified by recrystallization from ethanol. Their structures were examined using FT-IR and ^{1}H NMR spectroscopy, while elemental analysis was used to assess their chemical composition. The synthesized compounds were obtained in yields ranging from 74% to 88%, with **ANCH-6** giving the highest yield (88%) followed by **ANCH-5** (85%). The products varied in colour from pale yellow and yellow to straw-yellow and brown.

The FT-IR spectra of the synthesized derivatives exhibited absorption bands assigned to aromatic C–H stretching in the region of 3073.14-3019.28 cm^{-1} and aliphatic C–H stretching between 2961.34 and 2825.48 cm^{-1}. The carbonyl-associated absorption bands appeared between 1732 and 1705.63 cm^{-1}, which support the presence of carbonyl functionality in the synthesized compounds. Differences in the positions of these bands may be related to the substitution pattern and the molecular environment of the carbonyl group. The ^{1}H NMR spectra provided further structural information. The signals assigned to cyclohexanone ring protons occurred within the reported range δ 0.784-2.408 ppm, while the aliphatic chain protons appeared between δ 3.098 and 3.847 ppm. The aromatic proton signals extended across the region δ 6.926-8.534 ppm, consistent with the aromatic rings in the proposed structures. Substituent-related signals were reported at δ 2.78 ppm for the methoxy group in **ANCH-1** and δ 2.92 ppm for the methyl group in **ANCH-5**. The ^{13}C NMR spectra of the synthesized compounds exhibited two carbonyl carbon resonances in the ranges of δ 190.21-192.19 and 199.29-202.87 ppm. The cyclohexanone ring carbons C-1 and C-3 appeared at δ 53.82-55.97 and 37.18-41.11 ppm, respectively, while C-4, C-5 and C-6 resonated at δ 20.98-21.32, 21.31-21.79 and 28.16-30.97 ppm, respectively. The aliphatic chain carbon signals occurred within the ranges of δ 45.13-50.98 and 47.60-51.94 ppm. The substituent-related resonances varied according to the nature of the attached groups, while the aromatic carbon signals appeared across δ 113.69-155.16 ppm.

ADME prediction: All the **ANCH** compounds satisfied Lipinski's rule of five, with no violations. All compounds except **ANCH-2** exhibited TPSA values within the acceptable range. The predicted intestinal absorption exceeded 90% for most compounds, while **ANCH-2** showed an absorption value of 81.41%, which remains favourable. All compounds had a predicted bioavailability score of 0.55. Their predicted solubility values ranged from -6.53 to -5.85, which suggest the limited aqueous solubility. The predicted ADME properties of the synthesized **ANCH** compounds are shown in Table-1.

Pharmacokinetics and drug-likeness: The pharmacokinetic and drug-likeness profiles of the synthesized compounds **ANCH-1**, **ANCH-2** and **ANCH-4-8** were predicted using the SwissADME online tool. Most compounds were predicted to exhibit high gastrointestinal absorption, whereas **ANCH-7** showed low gastrointestinal absorption. None of the compounds was predicted to cross the blood-brain barrier (BBB). The cytochrome P450 inhibition profile revealed predicted inhibition of CYP2C9, CYP2C19 and CYP3A4 by all the compounds. **ANCH-2** was predicted to inhibit CYP1A2, while the remaining compounds showed no inhibition of this isoform. For CYP2D6, all compounds except **ANCH-2** were predicted to exhibit inhibitory activity (Table-2).

Drug-likeness was assessed using Lipinski's, Ghose, Veber, Egan and Muegge rules, together with bioavailability scores. Although the results were reported to indicate compliance with Lipinski's rule, **ANCH-2** and **ANCH-4–8** were listed as having one violation. All compounds satisfied Veber's rule without violations, whereas each compound had one violation under the Ghose, Egan and Muegge criteria. None of the compounds fully satisfied the Egan or Muegge rules. The medi-

TABLE-1
THE ADME VALUES OF THE SYNTHESIZED COMPOUNDS **ANCH 1-2, 4-8**

Compound	R	Log P	Mol. wt.	H-A	H-D	Mol. ref	Solubility	TPSA	% of Abs	Drug score
ANCH-1	4-OCH_3	3.67	386.48	3	0	116.86	-5.91	43.37	94.037	0.55
ANCH-2	4-NO_2	3.00	401.45	4	0	119.19	-6.53	79.96	81.41	0.55
ANCH-4	2-Cl	3.56	390.9	2	0	115.37	-6.4	34.14	97.222	0.55
ANCH-5	4-CH_3	3.62	370.48	2	0	115.33	-6.13	34.14	97.222	0.55
ANCH-6	4-H	3.45	356.46	2	0	110.36	-5.75	34.14	97.222	0.55
ANCH-7	4-Br	3.71	435.35	2	0	118.06	-6.46	34.14	97.222	0.55
ANCH-8	4-Cl	3.69	390.9	2	0	115.37	-6.4	34.14	97.222	0.55

TABLE-2
PHARMACOKINETICS PARAMETERS VALUES OF THE SYNTHESIZED COMPOUNDS **ANCH 1-2, 4-8**

Compound	GI adsorption	BBB permeant	P- glycoprotein substrate	CYPIA2 inhibitor	CYP2C19 inhibitor	CYP2C9 inhibitor	CYP2D6	CYP3A4
ANCH-1	High	No	Yes	No	Yes	Yes	Yes	Yes
ANCH-2	High	No	No	Yes	Yes	Yes	No	Yes
ANCH-4	High	No	Yes	No	Yes	Yes	Yes	Yes
ANCH-5	High	No	Yes	No	Yes	Yes	Yes	Yes
ANCH-6	High	No	Yes	No	Yes	Yes	Yes	Yes
ANCH-7	Low	No	Yes	No	Yes	Yes	Yes	Yes
ANCH-8	High	No	Yes	No	Yes	Yes	Yes	Yes

cinal assessment revealed no alerts in the PAINS filter, while **ANCH-1** and **ANCH-4–8** had no alerts in the Brenk filter. All compounds showed two lead-likeness violations associated with molecular weight higher than 350 and an XLOGP3 value above 3.5. The evaluated compounds exhibited three to four violations across the assessed drug-likeness criteria (Table-3).

Molecular docking: The synthesized **ANCH-1**, **ANCH-2** and **ANCH-4–8** compounds exhibited favourable binding affinity scores compared with the standard drug, with more negative docking scores corresponding to stronger predicted binding. Except for **ANCH-5**, the synthesized compounds showed better hydrogen-bonding interactions. **ANCH-2** formed two hydrogen bonds with the amino acid residues LYS A:319 and LYS A:115, which is found to be similar interactions observed for the standard drug. The binding affinity scores for the compounds were -9.1 and -9.4 kcal/mol. The docking profiles revealed favourable binding supported by hydrogen-bonding and hydrophobic interactions. These results are consistent with possible inhibition of bacterial cell-wall synthesis, although docking alone cannot confirm the mechanism of action. The docking scores and interactions of the compounds with protein 1UAG are given in Table-4, while the 2D and 3D interaction diagrams for ANCH-2 are shown in Fig. 1.

TABLE-3
MEDICINAL PROPERTY AND DRUG-LIKENESS RESULTS OF THE SYNTHESIZED COMPOUNDS **ANCH 1-2, 4-8**

Compound	Drug likeness						Medicinal chemistry			
	Lipinski's	Ghose	Veber	Egan	Muegge	Bioavailability	Pains	Brenk	Lead likeness	Synthetic availability
ANCH-1	Yes	1	Yes	No	No	0.55	0-alert	0-alert	No	3.25
ANCH-2	Yes	1	Yes	No	No	0.55	0-alert	1-alert	No	3.22
ANCH-4	Yes	1	Yes	No	No	0.55	0-alert	0-alert	No	3.42
ANCH-5	Yes	1	Yes	No	No	0.55	0-alert	0 -alert	No	3.22
ANCH-6	Yes	1	Yes	No	No	0.55	0-alert	0 -alert	No	3.12
ANCH-7	Yes	1	Yes	No	No	0.55	0-alert	0 -alert	No	3.32
ANCH-8	Yes	1	Yes	No	No	0.55	0-alert	0 -alert	No	3.27

TABLE-4
DOCKING RESULTs OF THE SYNTHESIZED COMPOUNDS **ANCH 1-2, 4-8** WITH 1UAG PROTEIN

Compounds	Docking score	H-B interaction	Hydrophobic interaction
ANCH-1	-9.0	LYS A:348, ASN A:138	LEU A:416, PHE A:422
ANCH-2	-9.4	LYS A:348, ARG A:302, LYS A:319, LYS A:115,	LEU A:416, PHE A:422
ANCH-4	-9.0	SER A:264, ASN A:268	PHE A:303
ANCH-5	-8.3	-	PHE A:303, LEU A:333, ARG A:302, LEU A:263, LEU A:299
ANCH-6	-8.5	ASN A:268	PHE A:303
ANCH-7	-9.0	ASN A:138, LYS A:348	LEU A:416, LYS A:319, HIS A:183, PHE A:422
ANCH-8	-8.9	SER A:264, ASN A:268	PHE A:303
Ciprofloxacin Std. drug	-7.8	LEU: 416, SER: 415, HIS: 183, LYS: 115, LYS: 319	LYS: 319, PHE: 422

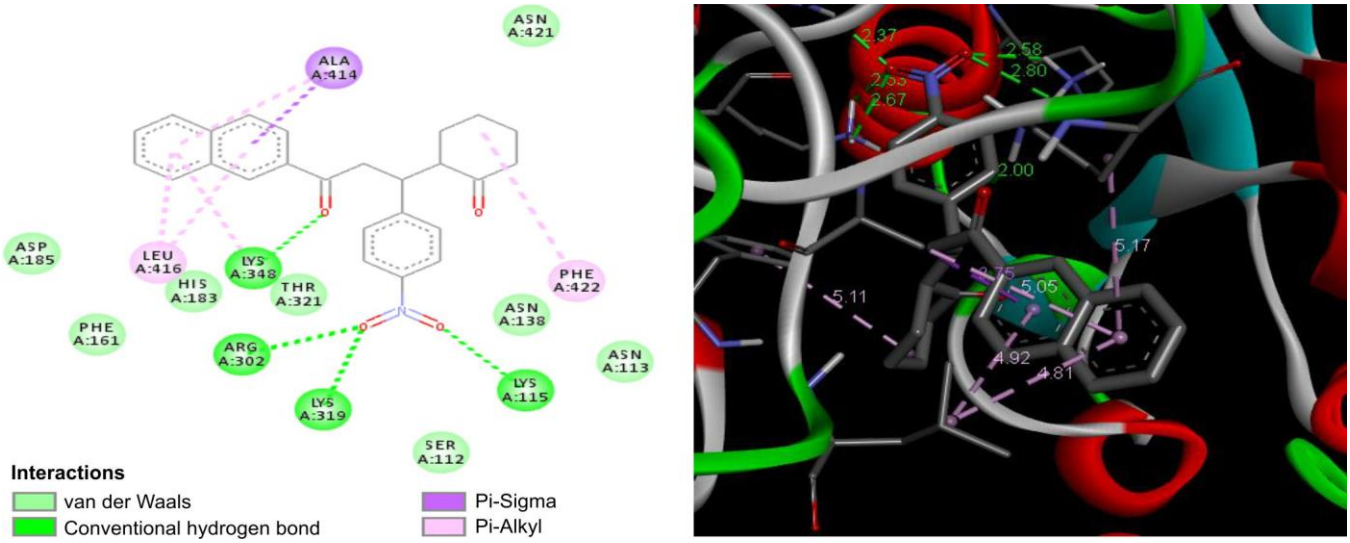


Fig. 1. 2D and 3D images of compound **ANCH-2** docked with 1UAG protein

Docking with 5KEE protein: The **ANCH** compounds were docked against the 5KEE protein and all compounds exhibited favourable binding affinity scores. **ANCH-4**, which contains a chloro substituent on the phenyl ring, showed the strongest predicted binding, with a docking score of -9.6 kcal/mol (Table-5). Each compound formed at least one hydrogen bond and displayed favourable hydrophobic interactions with the target protein (Fig. 2).

Docking with 5XZ0 protein: The **ANCH** compounds were docked against the 5XZO protein, and all compounds exhibited favourable binding affinity scores. **ANCH-2**, which contains a nitro substituent on the phenyl ring, showed the strongest predicted binding, with a docking score of -8.9 kcal/mol (Table-6). All compounds except **ANCH-7** formed at least one hydrogen bond. Favourable hydrophobic interactions were observed across the series (Fig. 3).

Docking result with 1OQA: Within the ANCH series, ANCH-2 formed hydrogen-bond interactions with the amino acid residues GLN A:73, ILE A:71, GLN A:104 and ILE A:105, with a binding affinity score of −7.9 kcal/mol. **ANCH-3** exhibited a binding affinity score of -7.1 kcal/mol. The compounds showed favourable hydrophobic interactions,

TABLE-5
DOCKING RESULTS OF SYNTHESIZED COMPOUNDS **ANCH 1-2, 4-8** WITH 5KEE PROTEIN

Compounds	Docking score	H-B interaction	Hydrophobic interaction
ANCH-1	-9.0	ARG A:35, ARG A:87, LYS A:84, TYR A:85	TYR A: 113, LEU A: 89, ASP A: 83
ANCH-2	-9.2	ARG A:87, ARG A: 35, TYR A: 85	TYR A: 113, LEU A: 89, ASP A: 83
ANCH-4	-9.6	ARG A:87, LYS A:84	ARG A:35
ANCH-5	-9.0	LYS A:84	ARG A:35, TYR A: 113, LEU A:37, LEU A: 89, ARG A: 87, ASP A: 83
ANCH-6	-9.2	ARG A:87, LYS A:84	ARG A:35, TYR A: 113, TYR A: 115, LEU A: 89
ANCH-7	-9.4	ARG A:87, LYS A:84	ARG A:35, TYR A: 113, TYR A: 115, LEU A: 89, ASP A: 83
ANCH-8	-9.5	LYS A:84	ARG A:35, TYR A: 113, TYR A: 115, LEU A: 89, ASP A: 83
Ciprofloxacin Std. drug	-7.8	LEU : 416, SER : 415, HIS : 183, LYS : 115, LYS : 319	LYS: 319, PHE: 422

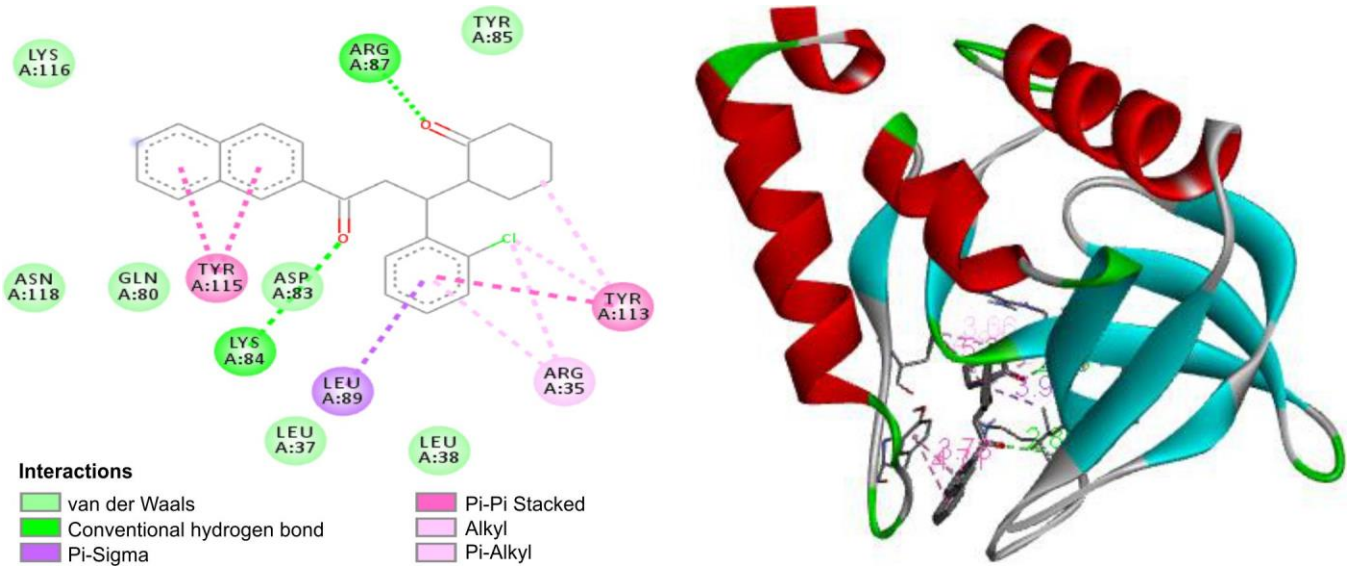


Fig. 2. 2D and 3D images of compound **ANCH-4** docked with 5KEE protein

TABLE-6
DOCKING RESULTS OF SYNTHESIZED COMPOUNDS **ANCH 1-2, 4-8** WITH 5XZ0 PROTEIN

Compounds	Docking score	H-B interaction	Hydrophobic interaction
ANCH-1	-8.3	ALA A:203	TYR A: 198, 213, LYS A: 212, ASP A: 199
ANCH-2	-8.9	HIS A:12, LYS A:207, ASP A:209	ASP A: 199, ALA A:203, LYS A:212, TRP A:197
ANCH-4	-8.0	GLU A:10, LEU a:11	TYR A:186
ANCH-5	-8.7	ASP A:199	ALA A:203, LYS A:212, PHE A:208, TRP A:197
ANCH-6	-8.6	HISA:12	ALA A:203, LYS A:212, TYR A:197
ANCH-7	-8.2	–	ARG A:35, TYR A: 113, TYR A: 115, LEU A: 89, ASP A: 83
ANCH-8	-8.5	HISA:12	ALA A:203, LYS A:212, PHE A:208, TRP A:197

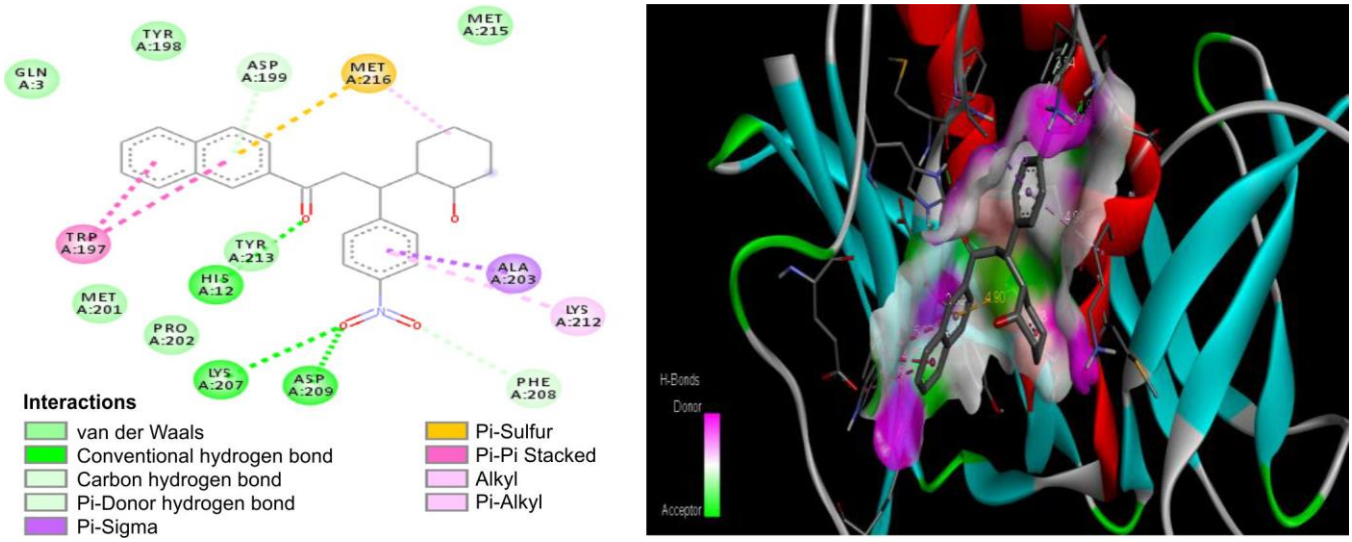


Fig. 3. 2D and 3D images of compound **ANCH-2** docked with 5XZ0 protein

TABLE-7
DOCKING RESULTS OF THE SYNTHESIZED COMPOUNDS **ANCH 1-2, 4-8** WITH 1OQA CANCER PROTEIN

Compounds	Docking score	H-B interaction	Hydrophobic interaction
ANCH-1	-7.4	–	HIS A:69, PRO A:59, PRO A:103, ILE A:102
ANCH-2	-7.9	GLN A: 73, ILE A: 71	HIS A:69, PRO A:103, PRO A;59
ANCH-4	-7.8	–	HIS A:69, PRO A:59, PRO A:103, ILE A:102
ANCH-5	-7.7	–	PRO A:59, ILE A:102, PRO A:103, ILEA:105
ANCH-6	-7.7	–	PRO A:103, PRO A:59, ILE A:102, HIS A:69
ANCH-7	-7.8	–	PRO A:59, PRO A:103, ILE A:102, HIS A:69
ANCH-8	-7.8	–	HIS A:69, PRO A:59, PRO A:103, ILE A:102

with binding affinity scores ranging from -7.4 to -7.8 kcal/mol (Table-7). The docking results suggest that the synthesized **ANCH** compounds have favourable interactions with the selected cancer-related protein (Fig. 4).

Antibacterial activity: The antibacterial activity of the **ANCH-1**, **ANCH-2** and **ANCH-4–8** compounds was evaluated against several bacterial strains using a standard reference method. A volume of 20 µL of each test solution was used for the antibacterial assay. The results revealed differences in the inhibitory activity of the synthesized compounds across the bacterial strains. **ANCH-4** and **ANCH-8** exhibited moderate to good inhibition across the tested bacterial panel, while three compounds showed comparatively stronger activity against *Bacillus megaterium* (Table-8). The observed

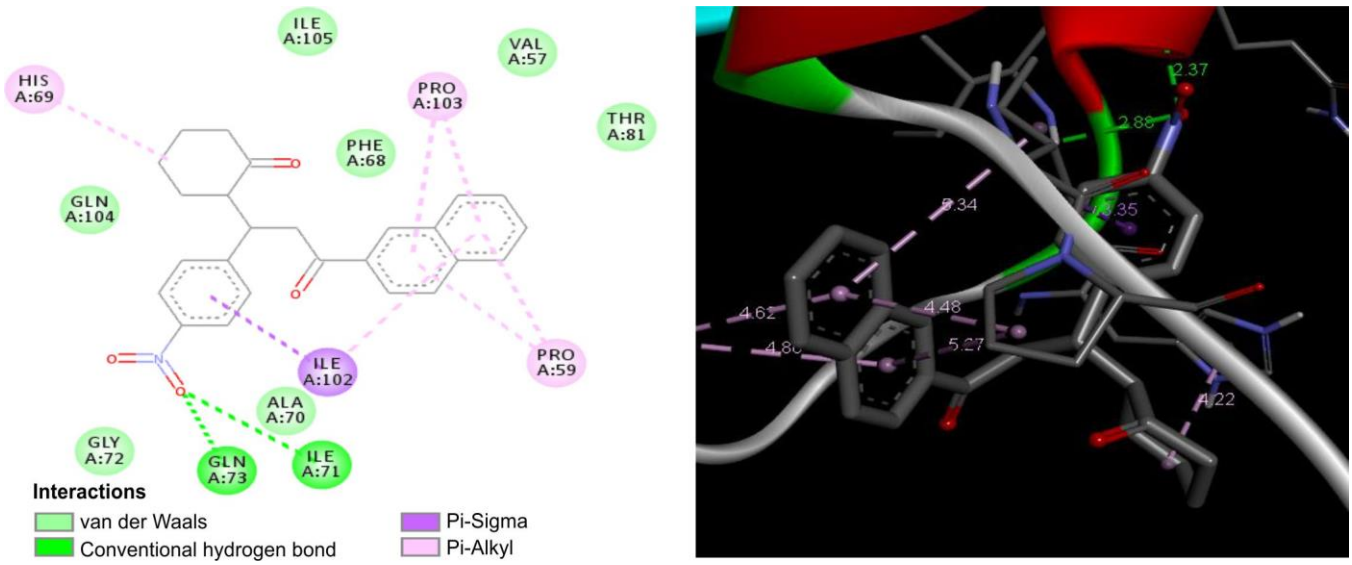


Fig. 4. 2D and 3D images of compound **ANCH-2** docked with 1OQA protein

TABLE-8
ANTIBACTERIAL RESULTs OF THE SYNTHESIZED COMPOUNDS **ANCH 1-2, 4-8**

Bacteria	**ANCH-1**	**ANCH-2**	**ANCH-4**	**ANCH-5**	**ANCH-6**	**ANCH-7**	**ANCH-8**
Enterobacteraerogenes	0	0	9	0	0	0	9
Citrobacterfreundii	0	0	10	0	0	0	9
Proteus vulgaris	0	0	7	0	0	0	8
Streptococcuslactis	0	0	7	0	0	0	7
Escherichia coli	0	0	9	0	0	0	8
Agrobacterium tumefaciens	0	0	10	0	0	0	11
Bacillus megaterium	0	0	14	0	0	0	12
Salmonella thyphimurium	0	0	8	0	0	0	8
Alcaligenesfaecalis	0	0	8	0	0	0	7
Listeriamonocytogenes	0	0	7	0	0	0	7
Erwiniachrysanthemi	0	0	9	0	0	0	8
Klebsiella pneumoniae	0	0	8	0	0	0	7
Shigella flexneri	0	0	9	0	0	0	9
Lactobacillusplantarum	0	0	14	0	0	0	12
Pseudomonas aeruginosa	0	0	9	0	0	0	9
Bacillus thuringiensis	0	0	12	0	0	0	11

variation in inhibition zones may be associated with differences in the chemical substituents and their influence on interactions with bacterial targets. The inhibition zones recorded for **ANCH-1**, **ANCH-2** and **ANCH-4–8** against the 16 bacterial strains are shown in Table-8.

Anticancer study: ANCH-4 compound was selected for anticancer screening against the MCF-7 human breast cancer cell line, with the human embryonic kidney (HEK) cell line used to assess its cytotoxicity toward non-cancerous cells. ANCH-4 exhibited an IC_{50} value of 33 ± 1.8 μM against MCF-7 cells, while its cytotoxicity value against HEK cells was 22 ± 0.6 μM. The standard drug doxorubicin showed a cytotoxicity value of 10 ± 1.2 μM against HEK cells. These results suggest that ANCH-4 may have a more favourable cytotoxicity profile in HEK cells than doxorubicin under the tested conditions. Its selectivity toward cancer cells requires further confirmation through comparative dose–response analysis and calculation of the selectivity index. The graphical representation of ANCH-4 activity against MCF-7 cells is shown in Fig. 5.

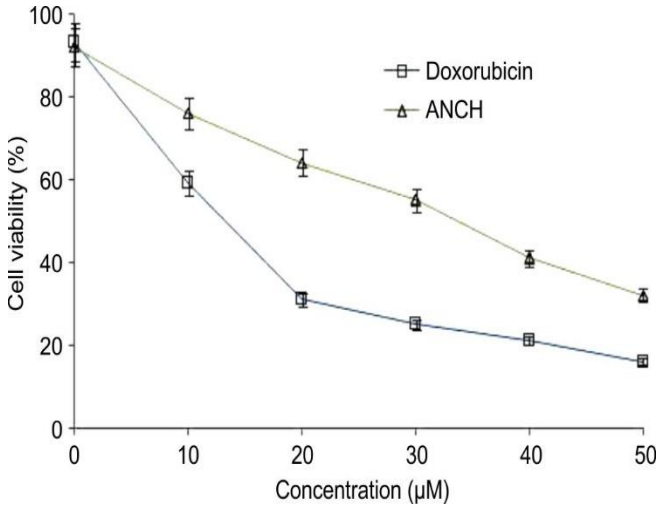


Fig. 5. Graphical representation of the cancer studies on MCF-7 cell lines of the compound **ANCH-4**

Conclusion

A series of cyclohexanone derivatives **ANCH-1**, **ANCH-2** and **ANCH-4–8**, was synthesized from the corresponding naphthyl chalcones and characterized using spectroscopic techniques. The compounds were evaluated through *in silico* ADME prediction, molecular docking and *in vitro* antibacterial and anticancer assays. ADME analysis indicated favourable predicted pharmacokinetic properties, although the compounds exhibited poor aqueous solubility and violations of certain drug-likeness criteria. **ANCH-4** and **ANCH-8** showed efficient antibacterial activity against the tested bacterial strains. Molecular docking against bacterial proteins (1UAG, 5KEE and 5XZO) and the cancer-associated protein 1OQA revealed favourable predicted binding affinities. **ANCH-4** was selected for anticancer evaluation against MCF-7 breast cancer cells and exhibited an IC_{50} value of 33 ± 1.8 μM, with comparatively lower toxicity towards HEK cells than doxorubicin under the tested conditions. These findings support further investigation of **ANCH-4** as a potential lead compound.

ACKNOWLEDGEMENTS

The authors are thankful to the management and Head of the Department of Chemistry, Karpagam Academy of Higher Education and Dr. N.G.P. Arts and Science College for providing the constant support for completed this work.

CONFLICT OF INTEREST

The authors declare that there is no conflicts of interest regarding the publication of this article.

DECLARATION OF AI-ASSISTED TECHNOLOGIES

During the preparation of this manuscript, the authors used an AI-assisted tool(s) to improve the language and no data, results or scientific conclusions were generated by AI. All analyses, interpretations and conclusions are the authors'

own. The authors reviewed and edited the content and take full responsibility for the published work.

REFERENCES

1. S. Ying, J. Wang, C. Xu, Y. Kang, X. Zhang, L. Shi, L. Fan, Z. Wang, J. Zhou, X. Wu, J. Wu, W. Li and G. Liang, *Russ. J. Gen. Chem.*, **86**, 2744 (2016); https://doi.org/10.1134/S1070363216120355
2. M.A.E.A. El-Hashash, S.M. Gomha and E.E. ElArab, *Chem. Pharm. Bull. (Tokyo)*, **65**, 90 (2017); https://doi.org/10.1248/cpb.c16-00759
3. S.R. Mousavi, *Chirality*, **28**, 728 (2016); https://doi.org/10.1002/chir.22653
4. S.M. Gomha, M.A. Abdallah, I.M. Abbas and M.S. Kazem, *Med. Chem.*, **14**, 344 (2018); https://doi.org/10.2174/1573406413666171020114105
5. A. Radwan, M. Khalid, H. Amer and M. Alotaibi, *Biointerface Res. Appl. Chem.*, **9**, 4642 (2019); https://doi.org/10.33263/BRIAC96.642648
6. R. Siegel, J. Ma, Z. Zou and A. Jemal, *CA Cancer J. Clin.*, **64**, 9 (2014); https://doi.org/10.3322/caac.21208
7. S. Parsai, R. Keck, E. Skrzypczak-Jankun and J. Jankun, *Oncol. Lett.*, **7**, 17 (2014); https://doi.org/10.3892/ol.2013.1679
8. X.L. Yu, T. Jing, H. Zhao, P.J. Li, W.H. Xu and F.F. Shang, *Asian Pac. J. Cancer Prev.*, **15**, 1465 (2014); https://doi.org/10.7314/APJCP.2014.15.3.1465
9. M.-C. Bourgeois-Daigneault, L.E. St-Germain, D.G. Roy, A. Pelin, A.S. Aitken, R. Arulanandam, T. Falls, V. Garcia, J.-S. Diallo and J.C. Bell, *Breast Cancer Res.*, **18**, 83 (2016); https://doi.org/10.1186/s13058-016-0744-y
10. H. Liu, Y.Z. Liu, F. Zhang, H.S. Wang, G. Zhang, B.H. Zhou, Y.L. Zuo, S.H. Cai, X.Z. Bu and J. Du, *Mol. Biosyst.*, **10**, 1320 (2014); https://doi.org/10.1039/C3MB70553F
11. L. Gianni, I. Panzini, S. Li, R.D. Gelber, J. Collins, S.B. Holmberg, D. Crivellari, M. Castiglione-Gertsch, A. Goldhirsch, A.S. Coates and A. Ravaioli, *Cancer*, **106**, 505 (2006); https://doi.org/10.1002/cncr.21651
12. H.A. Azim Jr., E. de Azambuja, M. Colozza, J. Bines and M.J. Piccart, *Ann. Oncol.*, **22**, 1939 (2011); https://doi.org/10.1093/annonc/mdq683
13. R.B. Badisa, S.F. Darling-Reed and P. Joseph, *Anticancer Res.*, **29**, 2993 (2009).
14. K. Begum, A. Ahmad and S. Tiwari, *Indian J. Chem.*, **60B**, 1490 (2021).
15. M.C. Ríos and J. Portilla, *Chemistry*, **4**, 940 (2022); https://doi.org/10.3390/chemistry4030065
16. I. Saleh, H. Raj KC, S. Roy, M.K. Abugazleh, H. Ali, D. Gilmore and M.A. Alam, *RSC Med. Chem.*, **12**, 1690 (2021); https://doi.org/10.1039/D1MD00230A
17. P.K. Mykhailiuk, *Chem. Rev.*, **121**, 1670 (2021); https://doi.org/10.1021/acs.chemrev.0c01015
18. S.M. Malik, B.H. Asghar, R. Syed, R.I. Alsantali, M. Morad, H.M. Altass, Z. Moussa, I.I. Althagafi, R.S. Jassas and S.A. Ahmed, *Front. Chem.*, **9**, 666573 (2021); https://doi.org/10.3389/fchem.2021.666573
19. B. Prabha and M.R. Ezhilarasi, *Biointerface Res. Appl. Chem.*, **11**, 9126 (2020); https://doi.org/10.33263/BRIAC112.91269138
20. M.N. Abdullah, P. Osw, S.A. Hassan and S. Othman, *J. Mol. Struct.*, **1301**, 137361 (2024); https://doi.org/10.1016/j.molstruc.2023.137361
21. V.A. Kuthe, P.B. Shamkuwar, M.S. Charde and R.D. Chakole, *Int. J. Biol. Pharm. Allied Sci.*, **11**, 2191 (2022); https://doi.org/10.31032/IJBPAS/2022/11.5.5961
22. D. Zelelew, M. Endale, Y. Melaku, T. Geremew, R. Eswaramoorthy, L.T. Tufa, Y. Choi and J. Lee, *Adv. Appl. Bioinform. Chem.*, **16**, 61 (2023); https://doi.org/10.2147/AABC.S403413
23. P.G. Kumdale and N.V. Shitole, *Orient. J. Chem.*, **38**, 198 (2022); https://doi.org/10.13005/ojc/380125
24. B. Addoum, B.E. Khalfi, S. Sakoui, R. Derdak, A. Elmakssoudi and A. Soukri, *Lett. Appl. Nanobioscience*, **11**, 3780 (2021); https://doi.org/10.33263/LIANBS113.37803801
25. P. Balakrishnan and E.M. Ramanathan, *Lett. Appl. Nanobioscience*, **10**, 2181 (2020); https://doi.org/10.33263/LIANBS102.21812190
26. G.S. Masaret, *ChemistrySelect*, **6**, 974 (2021); https://doi.org/10.1002/slct.202004304